

Facile synthesis of single-crystalline rutile TiO₂ nano-rods by solution method

Rehan DANISH, Faheem AHMED, Nishat ARSHI, M. S. ANWAR, Bon Heun KOO

School of Nano and Advanced Materials Engineering, Changwon National University,
Changwon, Gyeongnam, 641-773, Korea

Received 18 June 2013; accepted 20 March 2014

Abstract: A convenient and scalable technique for the synthesis of rutile titanium dioxide (TiO₂) nano-rods was presented by using bulk TiO₂ powder, sodium hydroxide (NaOH) and distilled water as raw materials. X-ray diffraction (XRD) and field emission scanning electron microscopy (FESEM) studies indicate that the prepared sample is crystalline and free from any impurities, however, it has no distinct shape and possesses a huge degree of agglomeration, and the average crystal size is around 40 nm. After annealing the sample at 600 °C for 2 h, it is observed through FESEM that nano-rods are formed. And XRD analysis shows that the nano-rods are single crystalline with distinct and smooth surfaces in different sizes with average length of about 1 μm and diameter of about 80 nm. Further UV-visible spectroscopy and Raman studies were conducted for the prepared sample and the band gap of the final product is found to be 3.40 eV.

Key words: TiO₂; nanorods; solution method; crystal growth; rutile

1 Introduction

Nano-scale structures are of great interest due to their unique properties and the possibility of their application in the field of nano-electronics [1] and several other possible applications [2–10], because this 1D metal-oxide nano-structures have been center of interest of many academic and industrial research groups. Among these metal-oxide nanostructures TiO₂ is one of the most studied materials because of its unique application in photo-voltaic devices and dye sensitized solar cells [11–13] owing to a wide band gap of about 3.0–3.2 eV [14]. And we know as a matter of fact that there are three distinct structural polymorphs of TiO₂ anatase, rutile and brookite, brookite however is the least characterized among three, and rutile has proven to be comparable to anatase in its properties only with an additional advantage of being more stable chemically and thermally and has a high refractive index [15]. Over the last forty years TiO₂ synthesis has been intensely investigated and there have been various methods employed for the synthesis of nanostructures, e.g. physical/chemical vapor deposition, sol-gel, hydrothermal, electro-templating methods have been widely used as

synthesis techniques and there are various reports that discuss the effects of synthesis techniques on the nano-structures [16–19]. Compared to vapor deposition methods, solution methods are more suitable for inexpensive mass production however the hydrothermal technique requires specialized equipment and a variable pressure gradient control which makes it a little expensive over the simple solution method and it is time intensive. KOLEN'KO et al [18] used hydrothermal synthesis for nanorods of titanium oxide; TSAI et al [16] demonstrated and explained the formation of Nanorods using hydrothermal method. KASUGA et al [20] also demonstrated the formation of nano-tubes by similar kind of method and the only drawback of these techniques being time intensive. In this work, an easy and scalable and a very less time demanding approach for synthesis of rutile TiO₂ nano-rods using solution method and the effect of annealing on the structural and morphological properties were reported.

2 Experimental

All the reagents involved in the experiments were of analytical grade and utilized as-received without further purification. In the experimental arrangement, 1:6 molar

ratio of bulk TiO₂ powder (<5 μm, 99.99% from Sigma Aldrich; 0.05 mol/L) to sodium hydroxide (NaOH, 99.99%, Sigma Aldrich; 1.0 mol/L) solution was made by dissolving in DI water 250 mL with mild stirring at room temperature in a 250 mL capacity glass beaker and the setup was placed over a hot plate at the temperature of 100 °C for 90 min under vigorous stirring. After 90 min the precipitate was collected and centrifuged at 3000 r/min for 5 min. This process was repeated 3 times using ethanol. The remainder was dried in a furnace at 80 °C for 12 h. Later after drying the substance was hand grinded in agate mortar with a pestle to make it into a powder form and was used for characterization. Half of the powder was subjected to annealing at 600 °C for 2 h and then it was characterized.

The phase purity of the obtained product was characterized using Phillips X'pert (MPD-3040) X-ray diffractometer with Cu K_α radiations ($\lambda=0.15406$ nm) operated at voltage of 40 kV and current of 30 mA. The XRD pattern was recorded within the scan range of 20°–80°. Field emission scanning electron microscopy (FESEM) images were obtained using a MIRA II LMH microscope with an operating voltage of 15 kV. The elemental composition of TiO₂ nano-rods was determined by energy dispersive X-ray spectroscopy (EDX, Inca Oxford, attached to the FESEM) with an operating voltage of 15 kV within the energy range of 0–10 keV. In order to get the phonon vibration study of the TiO₂ nano-rods, micro-Raman spectrometer (NRS-3100) was used with a 532 nm solid-state primary laser as an excitation source in the backscattering configuration at room temperature. Room temperature optical absorption spectrum was recorded in the range of 200–800 nm using a UV-Vis spectrophotometer (Agilent 8453).

3 Results and discussion

3.1 Structural studies

Figure 1 shows the XRD patterns of the as-prepared sample and the sample annealed at 600 °C for 2 h. The presence of (110) peak indicates that the obtained powder is rutile TiO₂. Comparing the XRD pattern with the standard JCPDS (89–4920) it can be observed that the prepared sample is free from any other phases of TiO₂ (anatase and brookite), and also there are no characteristic peaks depicting any impurities. The standard lattice parameters are $a=b=0.4584$ nm and $c=0.2953$, which are in agreement with the calculated values for our samples $a=b=0.4582$ nm and $c=0.2953$. The average crystallite size was calculated from the Scherrer equation [10].

$$\tau = K\lambda/(\beta \cos \theta) \quad (1)$$

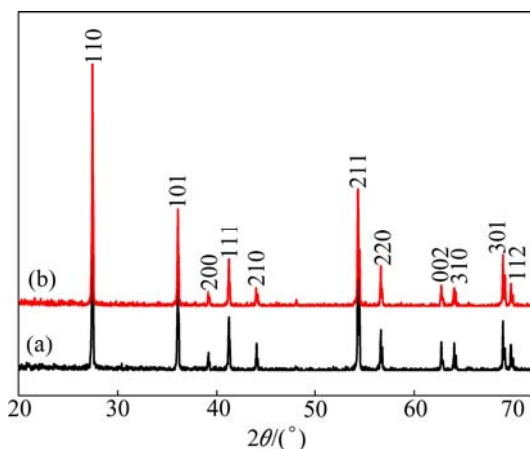


Fig. 1 XRD patterns of rutile TiO₂ as-prepared (a) and annealed at 600 °C for 2 h (b)

where τ is the mean size of the ordered (crystalline) domains, which may be smaller or equal to the grain size; K is a dimensionless shape factor, with a value close to unity. The shape factor has a typical value of about 0.9, but varies with the actual shape of the crystallite. λ is the X-ray wavelength, in this case it was Cu K_α radiation that has $\lambda=0.15406$ nm. β is the line broadening at half the maximum intensity (FWHM), after subtracting the instrumental line broadening, in radians. This quantity is also sometimes denoted as $A(2\theta)$. θ is the Bragg angle.

The crystallite size calculated from the Scherrer equation for the as-prepared sample was found to be about 40 nm and for the sample annealed at 600 °C for 2 h was found to be 52 nm.

Figure 2 shows the laser Raman spectra of TiO₂ taken at room temperature with a green (532 nm) laser in a back scattering mode for as prepared sample and the sample annealed at 600 °C for 2 h. The thermodynamically stable rutile phase TiO₂ exhibits major peaks at 242 cm⁻¹, 446 cm⁻¹ and 610 cm⁻¹ and minor peaks at 818 cm⁻¹, 707 cm⁻¹, and 319 cm⁻¹ [21–28]. Based on the space group D_{4h}¹⁴ for rutile and assumed site symmetries for the Ti and O atoms within the unit cell, group-theoretical analysis shows four Raman-active “lattice vibrations” assigned as follows: A_{1g}(610 cm⁻¹)+B_{1g}(144 cm⁻¹)+B_{2g}(827 cm⁻¹)+E_g(446 cm⁻¹) [22]. The peaks that are at 448 cm⁻¹(E_g), and 619 cm⁻¹(A_{1g}) in the as-prepared sample and the peaks at 447 cm⁻¹(E_g) and 609 cm⁻¹(A_{1g}) in the sample that is annealed at 600 °C for 2 h are attributed to Ti—O—Ti vibrations [21] and are the characteristic peaks of a rutile TiO₂ crystal system. The broad Raman peak at 242 cm⁻¹ and 234 cm⁻¹ in both the as-prepared and annealed samples are attributed either to the second order scattering or disorder effects. The Raman mode at 826 cm⁻¹ (B_{2g}) cannot be recorded due to its weak intensity. There is a blue-shift of the E_g mode between the

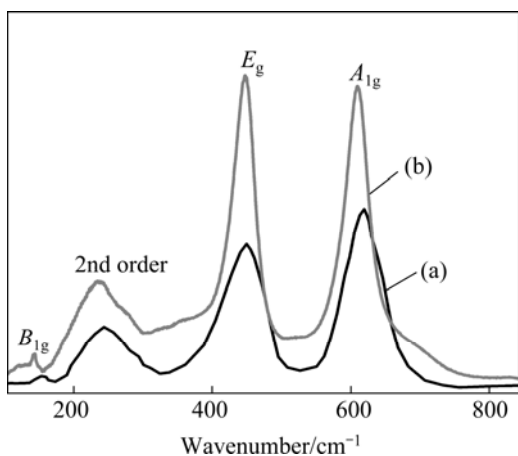


Fig. 2 Raman spectra of rutile TiO_2 as-prepared (a) and annealed at $600\text{ }^\circ\text{C}$ for 2 h (b)

the two samples that can be attributed to the Raman bands shift towards lower wave-number and their intensities relatively increase as the particle size also increases. The sharpness of the peaks and the intensity signify that the sample is highly crystalline and pure. Further the purity of the sample is substantiated by the EDX (Fig. 3(c)). The results of the Raman spectroscopy very well compliment the results that were obtained from XRD.

3.2 Morphological studies

From Fig. 3 it can be clearly seen that for the as-prepared sample (Fig. 3(a)) there is no distinct shape or morphology. But after we annealed the sample at $600\text{ }^\circ\text{C}$ for 2 h, there was a change in the morphology as shown in Fig. 3(b). There is a presence of nano-rods of nonuniform size distribution with an average length of about 1 μm and the average diameter of about 80 nm (aspect ratio of about 10). The change in the morphology from an agglomerated structure to the nanorods can be explained by the breaking of some Ti—O bonds of the TiO_2 precursor during the treatment with the concentrated NaOH solution, there is the formation of layered fragments that are intermediate phase between the formation of nano-tubes or nano-rod material [15]. The difference in the nano-tubes and nano-rods formation can be attributed to the techniques involved in the synthesis; some studies show that the use of hydrothermal method can result in the formation of nano-tubes as well as nano-rods [13, 15–16].

3.3 Optical properties

The changes in the optical properties of the as-prepared TiO_2 samples versus the annealed samples were evaluated by optical absorption spectra of TiO_2 samples at the wavelength range of 200–800 nm. The absorption spectrum of the sample annealed at $600\text{ }^\circ\text{C}$

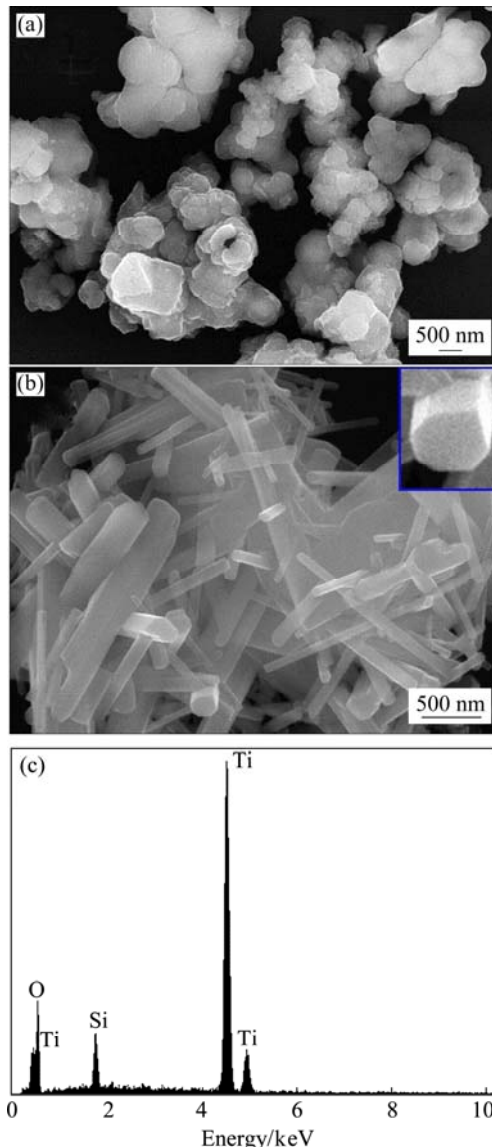


Fig. 3 FESEM images of rutile TiO_2 as-prepared (a) and annealed at $600\text{ }^\circ\text{C}$ for 2 h (b) and corresponding EDX spectrum of rutile TiO_2 (c)

shifts to longer wavelengths as compared with the as-prepared TiO_2 . This suggests that annealing effect is accompanied by a systematic low energy shift of the optical band gap. Since the inter-band transition in rutile phase TiO_2 is of direct type, the optical-absorption coefficient of rutile type TiO_2 can be expressed by [29].

$$(\alpha h\nu) = A(h\nu - E_g)^{1/2} \quad (2)$$

where A is a constant; $h\nu$ is the photon energy; E_g is the optical band-gap energy. Figure 4 shows the plots of $(\alpha h\nu)^2$ versus $(h\nu)$ for the as-prepared and annealed rutile TiO_2 nano-rods. The E_g values of the nano-rods were determined from the intercept of $(\alpha h\nu)^2$ versus $h\nu$ curves and found to be 3.75 eV for as-prepared TiO_2 however for the samples annealed at $600\text{ }^\circ\text{C}$ the E_g value was decreased to 3.40 eV. This decrease is attributed to the

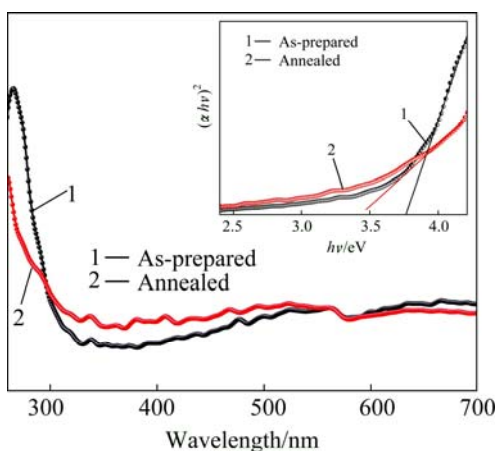


Fig. 4 Optical absorption spectra of TiO_2 and in inset plot of $(\alpha hV)^2$ versus hV

shrinkage effect of the optical band gap because of the increase in particle size.

3.4 Growth mechanism

The formation process can be understood on the basis of the obtained results in this work. When bulk TiO_2 is treated with NaOH aqueous solution, some of the $\text{Ti}—\text{O}—\text{Ti}$ bonds are broken and there is a molecular rearrangement and $\text{Ti}—\text{O}—\text{Na}$ and $\text{Ti}—\text{OH}$ bonds are formed. When the material is treated with distilled water, the $\text{Ti}—\text{O}—\text{Na}$ and $\text{Ti}—\text{OH}$ bonds are believed to react with water to form new $\text{Ti}—\text{O}—\text{Ti}$ bonds. At this stage there is a maximum probability of the rutile TiO_2 phase being formed because the precursor used was rutile. It also can be noted that during molecular recombination in the initial stirring the $\text{Ti}—\text{O}—\text{Na}$ bond that is formed is of layered structure and since numerous $\text{Ti}—\text{O}—\text{Na}$ bonds exist on the surface of TiO_2 , in a number so that the overall charge balance is maintained and except for residual microscopic charges. Therefore after the sample is annealed in order to avoid electrostatic repulsion of the residual charges a structure is formed in which the charges parts can be located as far away as possible from each other. Therefore, when the samples are treated with ethanol, the charged parts disappear gradually; the $\text{Ti}—\text{O}—\text{Na}$ bond may be converted into a $\text{Ti}—\text{OH}$ bond with a residual charged area. The $\text{Ti}—\text{OH}$ bond may form a sheet, which is contained in the rod structure. In addition, since the $\text{Ti}—\text{O}—\text{Ti}$ bonds or $\text{Ti}—\text{O}—\text{H}—\text{O}—\text{Ti}$ hydrogen bonds are generated through the dehydration of $\text{Ti}—\text{OH}$ bonds by annealing at 600°C for 2 h, the bond distance from one Ti to the next Ti on the surface decreases, and since the structure was already layered therefore during the heating process a slight residual electrostatic repulsion due to $\text{Ti}—\text{O}—\text{Na}$ bonds may lead to the formation of nano-rod.

4 Conclusions

A facile synthesis route for rutile TiO_2 nano-rods was investigated. And the optical properties were evaluated with the help of optical absorption spectra. With the solution route, nano-rods with length of about 1 μm and diameter of about 80 nm (aspect ratio of about 10) can be synthesized. It was found that the sample is indeed pure and free from any impurities. Raman shifting also explained the increase in size after annealing. Optical studies show that gap decreases after annealing which shows the possibility of the material being used in opto-electronic devices. The technique demonstrated is convenient and less expensive as compared to many other techniques.

Acknowledgement

This work is supported by the MKE (The Ministry of Knowledge Economy), Korea Under the ITRC (Information Technology Research Centre) support program supervised by the NIPA (National IT industry Promotion Agency) (NIPA-2012-H0301-12-2009), and also supported by the Ministry of Education, Science and Technology (MEST) and National Research Foundation of Korea (NRF) through the Human Resource Training Project for Regional Innovation (2012H1B8A2026212).

References

- [1] TANS S J, VERSCHUEREN A R M, DEKKER C. Room-temperature transistor based on a single carbon nanotube [J]. *Nature-London*, 1998, 393: 49–52.
- [2] YANG Ze-heng, ZHANG Yuan-cheng, ZHANG Wei-xin, WANG Xue, QIAN Yi-tai, WEN Xiao-gang, YANG Shi-he. Nanorods of manganese oxides: Synthesis, characterization and catalytic application [J]. *Journal of Solid State Chemistry*, 2006, 179: 679–684.
- [3] LAI T L, LAI Y L, LEE C C, SHU Y Y, WANG C B. Microwave-assisted rapid fabrication of Co_3O_4 nanorods and application to the degradation of phenol [J]. *Catalysis Today*, 2008, 131: 105–110.
- [4] WANG Yan, CAO Jian-liang, WANG Shu-rong, GUO Xian-zhi, ZHANG Jun, XIA Hui-jan, ZHANG Shou-min, WU Shi-hua. Facile synthesis of porous $\text{r}-\text{Fe}_2\text{O}_3$ nanorods and their application in ethanol sensors [J]. *J Phys Chem C*, 2008, 112: 17804–17808.
- [5] HU W K, GAO X P, GENG M M, GONG Z X, NOREUS D. Synthesis of CoOOH nanorods and application as coating materials of nickel hydroxide for high temperature Ni-MH cells [J]. *Journal of Physical Chemistry B Letters*, 2005, 109: 5392–5394.
- [6] SEOW Z L S, WONG A S W, THAVASI V, JOSE R, RAMAKRISHNA S, HO G W. Controlled synthesis and application of ZnO nanoparticles, nanorods and nanospheres in dye-sensitized solar cells [J]. *Nanotechnology*, 2009, 20: 045604.
- [7] CHON J W M, BULLEN C, ZIJLSTRA P, GU M. Spectral encoding on gold nanorods doped in a silica sol-gel matrix and its application to high-density optical data storage [J]. *Adv Funct Mater*, 2007, 17(6): 875–880.
- [8] AHMED F, ARSHI N, ANWAR M S, DANISH R, KOO B H.

- Mn-doped ZnO nanorod gas sensor for oxygen detection [J]. Current Applied Physics 2013, 13(2): 64–68.
- [9] AHMED F, KUMAR S, ARSHI N, ANWAR M S, KOO B H, LEE C G. Structural and magnetic properties of $Zn_{1-x}Co_xO$ nanorods prepared by microwave irradiation technique [J]. Journal of Nanoscience and Nanotechnology, 2012, 12: 1386–1389.
- [10] AHMED F, KUMAR S, ARSHI N, ANWAR M S, KOO B H, LEE C G. Rapid and cost effective synthesis of ZnO nanorods using microwave irradiation technique [J]. Functional Materials Letters, 2011, 4(1): 1–5.
- [11] SRINIVAS K, YESUDAS K, BHANUPRAKASH K, JAYATHIRTHA RAO V, GIRIBABU L. Combined experimental and computational investigation of anthracene based sensitizers for DSSC: Comparison of cyanoacrylic and malonic acid electron with-drawing groups binding onto the TiO_2 anatase (101) surface [J]. J Phys Chem C, 2009, 113: 20117–20126.
- [12] PALOMARES E, CLIFFORD J N, HAQUE S A, LUTZA T, DURRANT J R. Slow charge recombination in dye-sensitized solar cells (DSSC) using Al_2O_3 coated nanoporous TiO_2 films [J]. Chem Commun, 2002: 1464–1465.
- [13] QIAN Jiang-feng, LIU Ping, XIAO Yang, JIANG Yan, CAO Yu-liang, AI Xin-ping, YANG Han-xi. TiO_2 -coated multilayered SnO_2 hollow microspheres for dye-sensitized solar cells [J]. Adv Mater, 2009, 21: 3663–3667.
- [14] MADHUSUDAN REDDY K, MANORMA SUNKARA V, RAMACHANDRA REDDY A. Bandgap studies on anatase titanium dioxide nanoparticles [J]. Materials Chemistry and Physics, 2002, 78: 239–245.
- [15] MO S D, CHING W Y. Electronic and optical properties of three phases of titanium dioxide: Rutile, anatase, and brookite [J]. Physical Review B, 1995, 51: 19.
- [16] TSAI C C, TENG H. Structural features of nanotubes synthesized from NaOH treatment on TiO_2 with different post-treatments [J]. Chem. Mater. 2006, 18: 367–373.
- [17] ZHAO X B, LIU X Y, DING C X, CHU P K. In vitro bioactivity of plasma-sprayed TiO_2 coating after sodium hydroxide treatment [J]. Surface & Coatings Technology, 2006, 200: 5487–5492.
- [18] KOLEN'KO Y V, KOVNIK K A, GAVRILOV A I, GARSHEY A V, FRANTTI J, LEBEDEV O I, CHURAGLOV B R, van TENDELOO G. YOSHIMURA M. Hydrothermal synthesis and characterization of nanorods of various titanates and titanium dioxide [J]. J Phys Chem B, 2006, 110: 4030–4038.
- [19] LIMMER S J, CHOU T P, CAO G Z. A study on the growth of TiO_2 nanorods using sol electrophoresis [J]. Journal of Materials Science, 2004, 39(3): 895–901.
- [20] KASUGA T, HIRAMATSU M, HOSON A, SEKINO T, NIIHARA K. Titania nanotubes prepared by chemical processing [J]. Adv Mater, 1999, 11: 1307–1311.
- [21] TSAI C C, TENG H. Structural features of nanotubes synthesized from NaOH treatment on TiO_2 with different post-treatments [J]. Chem. Mater, 2006, 18: 367–373.
- [22] OCANA M, GARCIA-RAMOS J V, SERNA C J. Low-temperature nucleation of rutile observed by Raman spectroscopy during crystallization of TiO_2 [J]. J Am Ceram Soc, 1992, 75: 2010–2012.
- [23] HARDCASTLE F D. Raman spectroscopy of titania (TiO_2) nanotubular water-splitting catalysts [J]. Journal of the Arkansas Academy of Science, 2011, 65: 43–48.
- [24] KATIYARS R S, DAWSONS P, HARGREAVES M M, WILKINSON G R. Dynamics of the rutile structure 111. lattice dynamics, infrared and Raman spectra of SnO [J]. J Phys C: Solid St. Phys, 1971, 4: 2421–2431.
- [25] OCATIA M, FORNFIS V, GARCIA RAMOS J V, SERENA C J. Factors affecting the infrared and Raman spectra of rutile powders [J]. Journal of Solid State Chemistry, 1988, 75: 364–372.
- [26] BETSCH R J, PARK H L, WHITE W B, Raman spectra of stoichiometric and defect rutile [J]. Mat Res Bull, 1991, 26: 613–622.
- [27] SAMARA G A, PEERCY P S. Pressure and temperature dependence of the static dielectric constants and Raman spectra of TiO_2 (rutile) [J]. Physical Review B, 1973, 7(3): 1131–1148.
- [28] SWAMY V. Size-dependent modifications of the first-order Raman spectra of nanostructured rutile TiO_2 [J]. Physical Review B, 2008, 77: 195414.
- [29] AHMED F, KUMAR S, ARSHI N, ANWAR M S, KIM G W, HEO S N, BYON E S, LEE S H, LYU N J, KOO B H. Magnetic, optical and structural property studies of Mn-doped ZnO nanosheets [J]. Journal of Nanoscience and Nanotechnology, 2012, 12: 5464–5468.

单晶金红石型 TiO_2 纳米棒的湿法合成

Rehan DANISH, Faheem AHMED, Nishat ARSHI, M. S. ANWAR, Bon Heun KOO

School of Nano and Advanced Materials Engineering, Changwon National University,
Changwon, Gyeongnam, 641-773, Korea

摘要: 用 TiO_2 粉末、NaOH 和蒸馏水为原料合成金红石型 TiO_2 纳米棒。XRD 和 FESEM 分析表明，制备的样品为单晶且无杂质，其平均粒径约为 40 nm。当样品于 600 °C 退火 2 h 后，FESEM 观察发现生成了 TiO_2 纳米棒。XRD 分析表明纳米棒为单晶。纳米棒表面光滑，其长约为 1 μm，直径约为 80 nm。紫外和拉曼光谱研究表明，所制备样品的能带间隙为 3.40 eV。

关键词: TiO_2 ; 纳米棒; 湿法; 晶粒生长; 金红石

(Edited by You-ping YANG)